Representation of a complex Green function on a real basis: Generalization to a three-body system

Tieniu Li,[1] Bernard Piraux,[2] and Robin Shakeshaft[1]
[1]*Physics Department, University of Southern California, Los Angeles, California 90089-0484*
[2]*Laboratoire de Physique Atomique et Moleculaire, 2 Chemin du Cyclotron, B-1348 Louvain-la-Neuve, Belgium*
(Received 3 December 2002; published 19 May 2003)

We develop further a new method for employing a set of real basis functions to represent the Green function at energies in the continuum, without regard for the asymptotic boundary conditions. The method is based on the analyticity of the Green function with respect to its underlying time scale. The diagonalization of large matrices is unnecessary. Although a large complex symmetric linear system of equations must be solved, this can be done with high stability and efficiency by using a generalization of the Cholesky decomposition of real positive definite symmetric matrices. We present results of test applications to ^1S-wave electron scattering from a hydrogen atom and photodetachment of the negative hydrogen ion. The extension from two- to three-body collisions entails the use of projection operators to distinguish different groups of asymptotic channels.

DOI: 10.1103/PhysRevA.67.052704 PACS number(s): 34.80.−i, 31.15.−p

I. INTRODUCTION

There is no dearth of numerical methods for treating atomic collisions. The numerous *ab initio* nonperturbative techniques that can quantitatively account for many aspects of three-body atomic scattering include, for example, *R* matrix [1], *J* matrix [2], pseudostate close coupling [3], convergent close coupling [4], complex exterior scaling [5], spline methods [6], and approaches based on the numerical integration of the time-dependent Schrödinger equation [7]. Nevertheless, some features, especially those involving strong correlation, demand considerable computing resources for an adequate description, and the *ab initio* treatment of processes involving four or more particles still appears formidable. Furthermore, while one-photon breakup of a three-body system is well within the grasp of current state-of-the-art methods, multiphoton breakup—which is of interest in view of the development of intense high-frequency light sources—is only beginning to be tackled [8–11]. Consequently, it remains worthwhile to explore alternative numerical techniques which might require more modest resources. With an eye towards this goal, and mindful that a quasiclassical approach [12] also offers significant promise of efficiency, we extend in the present paper the development [13–15] of a fully quantum method which was implemented on a desktop computer for the application reported on here.

The primary merit of our approach is that a *real* discrete basis representation of the Hamiltonian H can be employed without regards for the asymptotic boundary conditions on the wave function. The basis must cover the ''interior'' region where the dynamics take place, and in this respect our method is similar to the *R*-matrix method; but a significant difference is that it is unnecessary to match the wave function to its asymptotic form in the ''exterior'' region. In the following sections we develop our method further, generalizing its applicability to a three-body system, with the inclusion of both closed-channel (Feshbach) and open-channel (shape) resonances, and both partial and complete breakup of the system. We present results of some test calculations carried out for two processes, ^1S wave electron scattering from a hydrogen atom and photodetachment of the negative hydrogen ion.

Our approach exploits the analyticity of the resolvent $G(E)\equiv 1/(E-H)$ with respect to its underlying time scale. During the time that the fragments of the system are interacting the wave function can be represented on a real basis of relatively modest size. Information at asymptotically large times—times for which an extremely large basis would be required to represent the wave function—can be obtained through analytic continuation with respect to the time. To accomplish this the resolvent is expressed by the following series [13]:

$$G(E)=e^{-t_\phi H}\left(\frac{1}{E}+it_\phi(2t_\phi H)\times\sum_{n=1}^{\infty}\frac{1}{n}\mathcal{I}_n(2Et_\phi)L_{n-1}^{(1)}(2t_\phi H)\right), \tag{1}$$

where $\hbar=1$, $t_\phi\equiv t_0e^{i\phi}$ is a complex unit of time, nt_ϕ plays the role of a continuous complex time, $L_{n-1}^{(1)}(z)$ is an operator-valued associated Laguerre polynomial of degree $n-1$, and the numerical coefficients $\mathcal{I}_n(z)$ can be determined using a simple recurrence relation (see below). The value of the temporal phase ϕ fixes the branch of $G(E)$. The ''physical'' energy sheet, on which the resolvent satisfies an outgoing-wave boundary condition in position space when E is real and positive, is $-\phi<\arg(E)<2\pi-\phi$ with $0<\phi<\pi$. A resonance pole at $E_{\rm res}$, say, lies on the physical sheet if $\phi>\arg(E_{\rm res})$.

The preceding series expansion of $G(E)$ was derived [13] from a consideration of the analytic properties of the correlation amplitude $C(t)\equiv\langle\psi|e^{-iHt}|\psi\rangle$, where $|\psi\rangle$ is any normalizable ket which represents a physically realistic localized wave packet. The spectrum of H is effectively bounded above since the asymptotically large-energy-components of the wave packet ψ play no significant role. Thus it takes a finite time, characterized by t_0, for the wave packet to evolve noticeably under the influence of H. An informal examination [13] of $C(t)$ indicates that it is an analytic function of t except for a pair of second-order branch-point singularities, one at $t=\infty$ and the other at some finite point on the positive

imaginary axis at a distance greater than, but of the order of, t_0 from the origin. [In addition, if $|\psi\rangle$ is not orthogonal to the bound-state and quasibound-state eigenkets of H, $C(t)$ has an essential singularity at $t=\infty$, a surmountable nuisance to which we return in the following section.] The branch points arise from the dichotomy posed by the arrow of time. Although the initial state of the system may be unambiguously defined at some finite point in time, the system can evolve either forwards or backwards, and the state at the single point $t=\infty$ depends on the direction of evolution to this point. The finite branch point, which is paired with the branch point at infinity, sets the time scale of the system's evolution. The presence of this finite branch point limits the radius of convergence of a Taylor-series expansion of $C(t)$ in powers of t to roughly t_0. However, we can map one half of the t plane, which excludes the finite branch point, onto a disk. Thus, we introduce the conformal transformation

$$t \to u = \frac{t + i t_0 e^{i\phi}}{t - i t_0 e^{i\phi}}, \tag{2}$$

which maps that half of the complex t plane below the line $\mathrm{Im}\, t/\mathrm{Re}\, t = \tan\phi$ onto the disk $|u|<1$. Noting that $\langle\psi|G(E)|\psi\rangle = -i\int_0^\infty dt\, e^{iEt} C(t)$, expanding $C(t)$ in (nonnegative) powers of u, and integrating term by term along a contour in the u plane which runs inside the unit circle from $u=-1$ $(t=0)$ to $u=1$ $(t=\infty)$, yields a series for $\langle\psi|G(E)|\psi\rangle$ which is equivalent to Eq. (1).

However, while we have eliminated the finite branch point, the branch point at infinity remains; the end point of integration at $u=1$ $(t=\infty)$ is a singularity and, consequently, the series is not formally convergent. Therefore, it (the series) must be analytically continued. A full account of the procedure for carrying this out has been given elsewhere [15], and so we only give an outline here—in Sec. II A—leaving the interested reader to turn Ref. [15] for the proof of various statements. However, in Ref. [15] we focussed on a two-body system [we used the series representation of $G(E)$ to calculate the second-order ac Stark shifts and widths of a hydrogen atom]. In applying the series representation to a three-body system it is necessary to distinguish between different asymptotic channels, or different groups of subchannel. This can be accomplished using projection operators, as described in Secs. II B and II C. In Sec. III we discuss the construction of these projection operators. In Sec. IV we present some results. We set $\hbar=1$.

II. FURTHER DETAILS

A. Series representation of *G(E)*

It is convenient to shift the spectrum of H by an amount Δ which is at least of the order of the ground-state binding energy, so that all eigenvalues of H are positive. The shift Δ characterizes the energy that can be exchanged between the fragments of the system. Recall that the real unit of time t_0 is the characteristic time it takes for the wave packet on which $G(E)$ acts to change appreciably when it evolves under e^{-iHt}. Roughly speaking, t_0 is the shorter of the time t_{stren} that characterizes the strength of the interactions between the fragments and the time t_{coll} that characterizes the duration of these interactions. To be specific, we define t_{coll} to be the shortest characteristic "collision" time $t_{\mathrm{coll}} \equiv 1/(E-\Delta_0)$, where Δ_0 is the position of the lowest threshold of the continuous spectrum, we define $t_{\mathrm{stren}} \equiv 1/\Delta$, and we define

$$t_0 \equiv \frac{1}{(1/t_{\mathrm{coll}}) + (1/t_{\mathrm{stren}})} \tag{3}$$

$$= \frac{1}{E + \Delta - \Delta_0}. \tag{4}$$

Note that E includes the shift Δ. If $E \gg \Delta - \Delta_0$ we have $t_0 \approx 1/E$. At high energies $t_0 \sim 0$ and $G(E) \approx 1/E$, in accord with Eq. (1).

Assume that $0<\phi<\pi$ (i.e., E lies on the "physical" sheet). For large n each coefficient $\mathcal{I}_n(2Et_\phi)$ behaves as a power series in $1/n$. If $\mathcal{I}_n(2Et_\phi)$ is replaced by this power series, truncated after a finite number of terms, the sum over n on the right side of Eq. (1) can be evaluated easily and (almost) exactly, despite its lack of formal convergence. However, the power series is only an asymptotic series; if it is subtracted from $\mathcal{I}_n(2Et_\phi)$ the remainder, denoted as $\mathcal{I}'_n(2Et_\phi)$, behaves as a decaying exponential, with exponent $i\sqrt{8nt_\phi E}$. When $\mathcal{I}_n(2Et_\phi)$ is replaced by this remainder the sum over n on the right side of Eq. (1) accounts for the energy-conserving scattering of flux; but unfortunately summation is not easy to perform—it is hindered by the lack of formal convergence, notwithstanding the exponential decay of $\mathcal{I}'_n(2Et_\phi)$.

The procedure for analytically continuing the sum depends on the magnitude of the eigenvalue spacing, in the vicinity of E, of each subchannel Hamiltonian. We elaborate further on this criterion below, but for the moment suppose that we are justified in performing the summation over the large-n terms by replacing $\mathcal{I}'_n(2Et_\phi)$ and $L^{(1)}_{n-1}(2t_\phi H)$ by their asymptotic forms. Here "large" n means $n \geqslant n_0$, where

$$n_0 \gg E t_0, \tag{5}$$

$$\sqrt{8 n_0 E t_0} \gg 1. \tag{6}$$

In this case we can write the sum over the large-n terms as

$$i t_\phi (2 t_\phi H) e^{-t_\phi H} \sum_{n=n_0}^{\infty} \frac{1}{n} \mathcal{I}'_n(2Et_\phi) L^{(1)}_{n-1}(2t_\phi H)$$

$$\approx -\frac{1}{2}\left(\frac{H t_\phi^2}{E^3}\right)^{1/4} (S_- + i S_+), \tag{7}$$

where the $S_\pm$ are the sums

$$S_\pm = i \sum_{n=n_0}^{\infty} \sqrt{\frac{2}{n}}\, e^{i\sqrt{8nt_\phi}(\sqrt{E} \pm \sqrt{H})}. \tag{8}$$

We replace the sum over n on the right side of Eq. (8) by an integral over n; the correction, given by the Euler-Maclaurin

formula, Ref. [16] is small (since $n_0 \gg 1$) and may be dropped. Integration over n yields

$$S_{\pm} = -\frac{e^{i\sqrt{8n_0 t_\phi}(\sqrt{E}\pm\sqrt{H})}}{\sqrt{t_\phi}(\sqrt{E}\pm\sqrt{H})}. \tag{9}$$

The result just obtained for S_+ is nonsingular and vanishes as n_0 increases. However, the same is not true for S_-; when the exponential $e^{-i\sqrt{8n_0 t_\phi H}}$ that appears in S_- acts on a continuum eigenvector of H it diverges as n_0 increases, and the divergence is amplified if E is close to the eigenvalue. Nevertheless, if $e^{-i\sqrt{8n_0 t_\phi H}}$ acts on a localized wave packet which is a superposition of continuum eigenvectors of H, the wave packet expands radially as it evolves under $e^{-i\sqrt{8n_0 t_\phi H}}$, with a radius proportional to $\sqrt{n_0 t_0}$; consequently, at any given point in position space the wave packet attenuates as $\sqrt{n_0 t_0}$ grows large. Hence, the right side of Eq. (9) vanishes as n_0 increases, and the series of Eq. (1) converges, when acting on a superposition of continuum eigenvectors. This remains true even if the wave packet includes bound-state eigenvectors. For suppose that the wave packet contains a bound-state eigenvector with eigenvalue $E_{\rm bd}$; since we are interested in values of E above the lowest threshold for fragmentation, we have $E > E_{\rm bd}$, and hence $e^{i\sqrt{8n_0 t_\phi}(\sqrt{E}-\sqrt{E_{\rm bd}})}$ vanishes as n_0 increases. Consequently, prior to integrating over n, we are free to reexpress the offending exponential in S_- on the right side of Eq. (8) as

$$e^{-i\sqrt{8nt_\phi H}} = e^{-i\sqrt{8nt_\phi^* H}} e^{i\sqrt{8nH}(\sqrt{t_\phi^*}-\sqrt{t_\phi})} \tag{10}$$

$$= e^{-i\sqrt{8nt_\phi^* H}} \sum_{m=0} \frac{i^m}{m!}[(e^{-i\phi}-1)\sqrt{8nHt_\phi}]^m. \tag{11}$$

We use Eq. (11) to modify the definition of S_- in Eq. (8), and again replace the sum over n by an integral to give, after integration,

$$S_- = -\frac{e^{i\phi}}{\sqrt{Ht_\phi}(\sqrt{Ee^{2i\phi}/H}-1)} \times \sum_{m=0} \frac{\Gamma[m+1,-i\sqrt{8n_0 t_\phi^*}(\sqrt{Ee^{2i\phi}}-\sqrt{H})]}{m!} \times \left(\frac{e^{i\phi}-1}{\sqrt{Ee^{2i\phi}/H}-1}\right)^m, \tag{12}$$

where $\Gamma(m+1,z)$ is the incomplete Γ function with the useful integral representation (which can be evaluated by the Gauss-Laguerre quadrature)

$$\Gamma(m+1,z) = e^{-z}\int_0^\infty dx (x+z)^m e^{-x}. \tag{13}$$

The sum over m on the right side of Eq. (12), which is the analytic continuation in the variable t_ϕ of the right side of Eq. (9), effectively amounts to an extrapolation from the complex energy $Ee^{2i\phi}$ to the real energy E. We note that a different scheme for extrapolation to the real energy axis was employed many years ago by McDonald and Nuttall [17].

The sum over the $n < n_0$ terms on the right side of Eq. (1) can be readily evaluated by using forward recursion for both the Laguerre polynomials and the numerical coefficients $\mathcal{I}_n(z)$. The Laguerre polynomials satisfy a standard recurrence relation, which can be started using $L_0^{(1)}(z)=1$ and $L_1^{(1)}(z)=2-z$. The $\mathcal{I}_n(z)$ satisfy the recurrence relation

$$n\mathcal{I}_{n+1} - 2(n-z/2)\mathcal{I}_n + n\mathcal{I}_{n-1} - 2(-1)^n i = 0, \tag{14}$$

which can be started using $\mathcal{I}_0(z) = 2i/z$ and $\mathcal{I}_1(z) = \mathcal{I}_0(z) + 2ie^{-z/2}E_1(-z/2)$.

When H is represented by a finite-dimensional matrix, the eigenvalue spectrum is discrete and consists of the bound-state eigenvalues together with a pseudocontinuum. The discreteness of the pseudocontinuum of H does not become apparent until a sufficiently large number of terms has been included in the sum over n on the right side of Eq. (1); the limit on n is roughly

$$n_{\rm max} \equiv \frac{1}{8(\delta H)^2 t_0}, \tag{15}$$

where $\delta\sqrt{H}$ is the spacing of the eigenvalues of $\sqrt{H}$ in the vicinity of $\sqrt{E}$. The replacement of the exponential $e^{-i\sqrt{8nt_\phi H}}$ by $e^{-i\sqrt{8nt_\phi^* H}}$, implemented in Eq. (11), ensures that the sum over n on the left side of Eq. (12) is effectively cut off after $n_{\rm cut}$ terms, where

$$n_{\rm cut} \equiv \frac{1}{2Et_0\phi^2}. \tag{16}$$

As long as

$$n_0 \ll n_{\rm cut}, \tag{17}$$

we can use the asymptotic forms of $\mathcal{I}_n'(2Et_\phi)$ and $L_{n-1}^{(1)}(2t_\phi H)$, and as long as

$$n_{\rm cut} \ll n_{\rm max}, \tag{18}$$

the discreteness of the pseudocontinuum remains hidden; in this case, the sum over m on the right side of Eq. (12) can be truncated after a finite number of terms—15 or less in the tests reported on here. Note that the condition $n_{\rm cut} \ll n_{\rm max}$ places a lower limit on the temporal phase ϕ. Indeed, it is apparent from the denominator $\sqrt{Ee^{2i\phi}/H}-1$ on the right side of Eq. (12) that the pseudocontinuum appears to be truly continuous if

$$\phi \gg 2(\delta\sqrt{H})/\sqrt{E}. \tag{19}$$

A necessary condition for the inequality $n_{\rm max} \gg n_0$ to be satisfied is given by substituting $n_{\rm max}$ for n_0 in Eq. (6), which yields $\delta\sqrt{H}/\sqrt{E} \ll 1$.

If $n_{\max} \not\gg n_0$ we cannot use the asymptotic forms of $\mathcal{I}'_n(2Et_\phi)$ and $L^{(1)}_{n-1}(2t_\phi H)$. In this case, in order to perform the analytic continuation in t_ϕ, we write

$$L^{(1)}_{n-1}(z) = ne^z[T^+_n(z) + T^-_n(z)], \tag{20}$$

where $T^+_n(z)$ and $T^-_n(z)$ are composed of outgoing and ingoing waves, respectively, in momentum space, plus a nonoscillating term that vanishes (as a power) as the momentum increases. The $T^\pm_n(z)$, and their derivatives with respect to $\sqrt{z}$, satisfy the recurrence relations

$$\begin{aligned}(n+1)\frac{d^m}{d\sqrt{z}^m}T^\pm_{n+1} - 2\left(n-\frac{z}{2}\right)\frac{d^m}{d\sqrt{z}^m}T^\pm_n + (n-1)\frac{d^m}{d\sqrt{z}^m}T^\pm_{n-1} \\ + 2m\sqrt{z}\frac{d^{m-1}}{d\sqrt{z}^{m-1}}T^\pm_n + m(m-1)\frac{d^{m-2}}{d\sqrt{z}^{m-2}}T^\pm_n \\ \pm\frac{\Gamma\left(n+\frac{1}{2}\right)}{\pi i n!}(\sqrt{z}\,\delta_{m0} + \delta_{m1}) = 0.\end{aligned} \tag{21}$$

Although $T^-_n(z)$ diverges as n increases (when $\phi \neq 0$) we can analytically continue $T^-_n(z)$ from z^* to z:

$$T^-_n(z) = \sum_{m=0} \frac{(\sqrt{z} - \sqrt{z^*})^m}{m!}\left(\frac{d^m}{d\sqrt{z}^m}T^+_n(z)\right)^*, \tag{22}$$

where only a finite number of derivatives are to be retained. The smaller is ϕ, the fewer the number of derivatives that must be included. In the tests reported on in Sec. IV we included six or fewer derivatives.

Recursion is now done in the backward direction, for both the $\mathcal{I}_n(z)$ and the $T^\pm_n(z)$ and their derivatives. Since there is an exponentially small component at large n, whose value is difficult to assess, the solutions obtained from backward recursion must be matched to the exact solutions at a smaller value of n. The matching for $\mathcal{I}_n(z)$ can be done at $n=0$, but the matching for the $T^\pm_n(z)$ and their derivatives should be done at a value of n much larger than 1 (for a reason given shortly). To accomplish this we make use of

$$\begin{aligned}\frac{d^m}{d\sqrt{z}^m}T^\pm_n(z) = \frac{1}{2n}\sum_{k=0}^{m}(-1)^k\binom{m}{k}\Bigg[e^{-z}H_k(\sqrt{z})L^{(1,m-k)}_{n-1}(z) \\ \pm\frac{i}{\sqrt{\pi}}\int_0^1 dx(1-x^2)^{m-1/2}H_{k+1}(\sqrt{(1-x^2)}z) \\ \times L^{(3/2,m-k)}_{n-1}((1-x^2)z)e^{-(1-x^2)z}\Bigg],\end{aligned} \tag{23}$$

where $H_n(z)$ is a Hermite polynomial of degree n and where $L^{(\alpha,k)}_n(z)$ is the kth derivative with respect to $\sqrt{z}$ of the associated Laguerre polynomial $L^{(\alpha)}_n(z)$. The integrals can be evaluated by the Gauss-Jacobi quadrature.

For $n \gg 1$, Et_0 the $T^\pm_n(z)$ depend on n through the combination nz. Thus m-th derivatives of $T^\pm_n(z)$ with respect to $\sqrt{z}$ contain terms which are amplified by $\sqrt{n}^m$. This could lead to intolerable roundoff error in the recursion of Eq. (21), a situation we avoid by matching at a suitably large value of n.

The maximum number, $n_{\max}$, of terms which can be included in the series representation of $G(E)$ without the discreteness of the pseudocontinuum of H becoming apparent is inversely proportional to the square of the energy spacing of the eigenvalues of H in the neighborhood of E. In general, this number depends on the asymptotic channel into which the fragments of the system separate. Typically, when a discrete basis is used to represent the wave function of a three-body system the eigenvalue spacing is smallest for the total-breakup channel. Thus, it is useful to divide the eigenvalue spectrum into two or more portions, each associated with a specific set of asymptotic channels. This can be accomplished by using projection operators, within the Feshbach formalism.

B. Projection operators

We take as our prototype three-body system two identical particles—electrons, to be specific—moving in the field of a stationary infinitely massive nucleus. Let $P_\alpha, P_{\alpha'}, \ldots$ be projection operators which are symmetric with respect to the interchange of the two electrons and which project onto orthogonal subspaces, each of which corresponds to a channel, or a group of subchannels, that is *open*, i.e., energetically accessible. We have

$$P^2_\alpha = P_\alpha, \tag{24}$$

$$P_\alpha P_{\alpha'} = P_{\alpha'} P_\alpha = 0, \tag{25}$$

where $\alpha, \alpha', \ldots$ are the collective quantum numbers which label open channels (or groups of subchannels). For the purpose of obtaining a useful representation of $G(E)$ we introduce the simpler resolvents

$$G_\alpha(E) = 1/(E - P_\alpha H P_\alpha), \tag{26}$$

$$G_0(E) = 1/(E - H_0), \tag{27}$$

where E lies in the continuous part of the spectrum of H and where H_0 is a Hamiltonian that differs from H by a perturbation W that only weakly couples together eigenstates of H with eigenvalues close to E. Here the term ''weakly couples'' means that the expectation value of W, with respect to any eigenket of H whose eigenvalue is close to E, is finite [18].

The full resolvent $G(E)$ can be expressed in terms of $G_0(E)$ as

$$G(E) = G_0(E)[M(E)]^{-1}G_0(E), \tag{28}$$

an identity which is eminently suited to computation, since the operator

$$M(E) \equiv G_0(E) - G_0(E)WG_0(E) \tag{29}$$

is symmetric and, owing to our restriction on the perturbation W, has a well-defined inverse. To prove this last remark we need to show that the eigenvalues of $M(E)$ are nonzero.

To this end suppose that $M(E)$ does have an eigenvalue which vanishes; let $|0\rangle$ be the eigenvector. Writing $M(E) = G_0(E)(E-H)G_0(E)$ we see that $(E-H)G_0(E)|0\rangle = 0$. Hence, adding $i\eta$ to E so as to avoid singularities, where η is positive but infinitsimal, $G_0(E+i\eta)|0\rangle$ must be an eigenvector of H with eigenvalue E, i.e., $G_0(E+i\eta)|0\rangle = |\Phi_E^+\rangle$, where $(E-H)|\Phi_E^+\rangle = 0$. Consequently, $M(E+i\eta)|0\rangle = i\eta G_0(E+i\eta)|\Phi_E^+\rangle$, and using the Lippmann-Schwinger equation

$$|\Phi_E^+\rangle = |\Phi_{0E}\rangle + G_0(E+i\eta)W|\Phi_E^+\rangle, \tag{30}$$

where $(E-H_0)|\Phi_{0E}\rangle = 0$, it follows that

$$M(E+i\eta)|0\rangle = |\Phi_{0E}\rangle + i\eta[G_0(E+i\eta)]^2 W|\Phi_E^+\rangle. \tag{31}$$

The second term on the right side of Eq. (31), which contains η as a factor, vanishes since $[G_0(E+i\eta)]^2 W|\Phi_E^+\rangle$ is finite, a consequence of the restriction that W does not strongly couple $|\Phi_E^+\rangle$ to itself. The first term on the right side of Eq. (31) does not vanish, and therefore we have a contradiction; thus $M(E)$ cannot have an eigenvalue that is zero.

It follows that the relevant branch points of $G(E)$ are contained entirely in $G_0(E)$. In particular, the "physical" branch of $G(E)$ is defined by $G_0(E)$. This permits us to apply our series expansion to a resolvent that is much simpler than $G(E)$. A suitable definition of H_0 is

$$H_0 = \sum_\alpha P_\alpha H P_\alpha, \tag{32}$$

where the sum is over all channels or groups of (sub)channels that are open. The perturbation is

$$W = \sum_\alpha \sum_{\alpha' \neq \alpha} P_\alpha H P_{\alpha'} + \sum_\alpha (P_\alpha HQ + QHP_\alpha) + QHQ, \tag{33}$$

where Q is the orthogonal projection operator

$$Q \equiv 1 - \sum_\alpha P_\alpha. \tag{34}$$

Noting that $P_\alpha H P_\alpha$ and $P_{\alpha'} H P_{\alpha'}$ commute—since P_α and $P_{\alpha'}$ are orthogonal—we can express $G_0(E)$ in the form

$$G_0(E) = \sum_\alpha P_\alpha G_\alpha(E) P_\alpha + Q/E. \tag{35}$$

The merit of Eq. (35) is that each of the partial resolvents $P_\alpha G_\alpha(E) P_\alpha$ has a rank (number of nonzero eigenvalues) far smaller than the rank of $G(E)$; furthermore, $P_\alpha G_\alpha(E) P_\alpha$ can be replaced by a series representation with its own special temporal phase, and, indeed, its own special time scale, which depends on the eigenvalue spacing of $P_\alpha H P_\alpha$ in the vicinity of E. Thereby, we obtain with relatively modest effort a representation of $G_0(E)$.

In fact, the effort required to construct the partial resolvents is less than implied so far. Only those eigenvectors of $P_\alpha H P_\alpha$ with eigenvalues close to E are needed to provide an adequate approximation to the energy-conserving part of $P_\alpha G_\alpha(E) P_\alpha$. Thus, *after* selecting the eigenvectors of $P_\alpha H P_\alpha$ with eigenvalues close to E we redefine P_α so that it projects only onto the smaller subspace containing these preferred eigenvectors. The discarded eigenvectors of $P_\alpha G_\alpha(E) P_\alpha$, which do not need to be calculated, are included in the Q subspace where they contribute to the non-energy-conserving part (the "principal part") of $G(E)$. To determine $G(E) = G_0(E) M^{-1}(E) G_0(E)$, or rather its action on some ket, we must solve an equation of the form $M(E)|a\rangle = |b\rangle$ where, using Eqs. (29), (33), and (35),

$$M(E) = \frac{Q}{E} - \frac{QHQ}{E^2} - \frac{1}{E}\sum_\alpha [P_\alpha G_\alpha(E) P_\alpha HQ + QHP_\alpha G_\alpha(E) P_\alpha] + \sum_\alpha P_\alpha G_\alpha(E) P_\alpha - \sum_\alpha \sum_{\alpha' \neq \alpha} P_\alpha G_\alpha(E) P_\alpha H P_{\alpha'} G_{\alpha'}(E) P_{\alpha'}. \tag{36}$$

Once $M(E)$ is represented by a matrix, we are faced with a complex symmetric system of linear equations whose solution can be determined efficiently, and with high stability, by expressing $M(E)$ as $L^t(E)L(E)$ where $L(E)$ is a *complex* lower triangular matrix, with $L^t(E)$ being its transpose; this is a generalization of the standard Cholesky decomposition [19] for a *real positive definite* matrix. The reason that it is possible to write $M(E) = L^t(E)L(E)$ is as follows: We can analytically continue $M(E)$ along a path which passes to the left along the upper edge of the real E axis to the region of the real energy axis below where the bound-state poles lie. In this region $-M(E)$ is real, symmetric, and positive definite, and therefore $-M(E)$ has the standard Cholesky decomposition, which, by absorbing a factor of i in L, we can reexpress as $M(E) = L^t(E)L(E)$. Since $M(E)$ remains symmetric, and since, by construction, no eigenvalues of $M(E)$ encircle a zero along the path that is followed in the E plane, we can analytically continue the relationship $M(E) = L^t(E)L(E)$ back to values of E in the continuum. The Hamiltonian QHQ that appears in the perturbation W on the right side of Eq. (33) need not be diagonalized. However, if QHQ is diagonalized L is (or can be arranged to be) highly sparse, so that the solution of the linear system simplifies enormously.

The presence of a resonance pole close to the real energy E requires special consideration. In performing the analytic continuation of the series expansion we assumed that the (partial) resolvent acts on a wave packet whose energy distribution in the vicinity of E includes only continuous components; but a quasibound state with a narrow width is hardly distinguishable from a true bound state in the continuum. There are two types of resonances, closed-channel (Feshbach) and open-channel (shape) resonances. Assume that P projects onto the subspace corresponding to all those subchannels that are open at energy E; thus $Q = 1 - P$

projects onto the closed-channel space. A closed-channel resonance originates from a bound state of QHQ. This discrete, localized state becomes unstable through the coupling $QHP+PHQ$, but it is stable at zeroth order in this coupling. Of course, the division of the full vector space into P and Q subspaces is somewhat arbitrary, and as the Q subspace is enlarged the P subspace must shrink. However, as long as the coupling $QHP+PHQ$ remains small a bound state of QHQ remains localized as the Q-subspace is enlarged. Hence closed-channel resonances are absent from the spectrum of PHP. Consequently, $P(E-PHP)^{-1}P$ can be replaced by its series expansion without further consideration. On the other hand, an open-channel resonance originates from a *non*localized eigenstate of PHP; there is no ''zeroth-order'' limit in which an open-channel resonance can be described by a localized eigenstate. On the contrary, in the lowest approximation, an open-channel resonance is represented by a superposition of nearly degenerate (pseudo)continuum eigenstates of $P_{\rm res}HP_{\rm res}$, where $P_{\rm res}$ projects onto the subspace corresponding to the open subchannel in which the resonance originates. Only those eigenvectors of $P_{\rm res}HP_{\rm res}$ whose eigenvalues lie close to the resonance, within a distance of the order of the resonance width, need to be included, but the spacing of these eigenvalues must be small compared to the resonance width so that there is a sufficient number of eigenstates to accurately describe the resonance. As long as this is the case, a temporal phase can be assigned to the resonance channel which is less than $\arg(E_{\rm res})$, thereby ensuring that the resonance does not lie on the physical sheet. Consequently, the resonance is excluded from the physical branch of $P_{\rm res}(E-P_{\rm res}HP_{\rm res})^{-1}P_{\rm res}$, and this partial resolvent can be replaced by its series expansion. We introduce another operator, $P_{\rm bg}$, which projects onto the ''background'' subspace correpsonding to those open subchannels not included in the ''resonance'' subspace. Since the resonance is absent from the spectrum of $P_{\rm bg}HP_{\rm bg}$ we can directly replace $P_{\rm bg}G_{\rm bg}(E)P_{\rm bg}$ by its series expansion.

C. Transition rate

We label the two electrons as 1 and 2, and denote the interaction between them as U_{12}. We denote the (internal or external) perturbation in the entrance channel as V. If $|\psi\rangle$ represents the initial state of the system, the response of the system to V is represented by

$$|\Psi\rangle = G(E)V|\psi\rangle, \tag{37}$$

where E is the total energy (including the photon energy if V describes one-photon absorption) of the system. In this subsection we consider the rate Γ_α for the system to undergo a transition to the open (sub)channel α. We express Γ_α in a form which requires only the response ket $|\Psi\rangle$ as input.

The symmetric operator which projects onto the subspace corresponding to (sub)channel α is [20]

$$P_{1\alpha}+P_{2\alpha}-P_{1\alpha}P_{2\alpha},$$

where $P_{i\alpha}$ for $i=1,2$ is the operator which projects onto the subspace in which a particular electron, the ith, has the energy range and other single-particle quantum numbers specified by the index α. By first expressing the rate in terms of the flux through the surface of a hypersphere of asymptotically large radius we showed elsewhere [21] that

$$\Gamma_\alpha = -2\,\mathrm{Im}\sum_{i=1}^{2}\{\langle\psi|V^\dagger P_{i\alpha}|\Psi\rangle + \langle\Psi|U_{12}P_{i\alpha}|\Psi\rangle\}. \tag{38}$$

The omission of the cross term $P_{1\alpha}P_{2\alpha}$ in this expression for the rate is a consequence of energy conservation, which is satisfied on a hypersphere of asymptotically large radius. One of the electrons residing on this hypersphere must have an energy less than $E/2$, but the cross term projects onto a subspace in which both electrons have energies in the same range, and in which, therefore, the total energy of the electrons is less than E; but this is prohibited by energy conservation.

Each of the two terms on the right side of Eq. (38) can be given a simple physical interpretation: The first term is the transition rate in the absence of final-state correlation, while the second term is the correction due to final-state correlation. Here we define the final-state (complex) correlation energy to be the expectation value with respect to the response ket $|\Psi\rangle$ of the non-Hermitian interaction $\Sigma_{i=1}^{2}Q_{i\alpha}U_{12}P_{i\alpha}$, where $Q_{i\alpha}=1-P_{i\alpha}$ and $Q_{i\alpha}P_{i\alpha}=0$. Since $P_{i\alpha}$ and U_{12} are each Hermitian, $\langle\Psi|P_{i\alpha}U_{12}P_{i\alpha}|\Psi\rangle$ is real, and therefore we can replace $\langle\Psi|U_{12}P_{i\alpha}|\Psi\rangle$ by $\langle\Psi|Q_{i\alpha}U_{12}P_{i\alpha}|\Psi\rangle$ on the right side of Eq. (38) to give

$$\Gamma_\alpha = -2\,\mathrm{Im}\sum_{i=1}^{2}\{\langle\psi|V^\dagger P_{i\alpha}|\Psi\rangle + \langle\Psi|Q_{i\alpha}U_{12}P_{i\alpha}|\Psi\rangle\}. \tag{39}$$

In the first of the two terms on the right side of Eq. (39) the perturbation V acts in a spatial region whose linear dimensions are of the order of the initial bound-state radius. This term describes the direct excitation by V of the system to (sub)channel α; it does not take into account the possibility that the system is directly excited by V to (sub)channels other than α, after which—and perhaps over distances far larger than the initial bound-state radius—the system migrates to (sub)channel α under the influence of the correlation interaction $\Sigma_{i=1}^{2}Q_{i\alpha}U_{12}P_{i\alpha}$. It is the second of the two terms on the right side of Eq. (39) which takes into account this indirect excitation of the system to (sub)channel α.

There would be no correlation, and obviously the second term on the right side of Eq. (39) would vanish, if U_{12} were to vanish. However, even though U_{12} does not vanish correlation can be small, particularly if the main effect of U_{12} is to screen one of the electrons from the nucleus, an effect which should not be attributed to correlation. We conclude this section by confirming that final-state correlation vanishes when one electron maximally screens the other electron from the nucleus. Let U_2 be the limit of U_{12} as electron 1 moves infinitesimally close to the nucleus. Since $P_{1\alpha}$ commutes with the central potential U_2 we have $[P_{1\alpha},U_{12}]=[P_{1\alpha},U_{12}-U_2]$. The presence of $P_{1\alpha}$ in the term $\langle\Psi|Q_{1\alpha}U_{12}P_{1\alpha}|\Psi\rangle$ ensures that in the final-state electron 1

remains closer to the nucleus than electron 2, so $U_{12}-U_2$ is a relatively weak interaction. In the limit of maximum screening, where U_{12} approaches U_2, $P_{1\alpha}$ commutes with U_{12} and therefore $\langle\Psi|Q_{1\alpha}U_{12}P_{1\alpha}|\Psi\rangle$ vanishes. Similarly, in the limit of maximum screening $\langle\Psi|Q_{2\alpha}U_{12}P_{2\alpha}|\Psi\rangle$ vanishes.

III. PROJECTION ONTO TWO-BODY STATES

We begin by constructing an operator that projects onto a subspace corresponding to some or all of those asymptotic channels in which one electron—say, for definiteness, electron 1—remains localized near the nucleus with an energy less than some upper limit, $e_{\max}$ say, where $e_{\max}$ is real but otherwise unspecified. We ignore the interaction of electron 2 with electron 1 and with the nucleus. The two electrons are tied through their angular momentum coupling, with L being the total angular-momentum quantum number. Aside from this coupling, electron 2 plays no role in the construction of the projection operator; it behaves like an infinitely massive, stationary, etherial (noninteracting) particle which carries angular momentum but no kinetic energy. Thus, we replace the Hamiltonian of electron 2 by

$$0_2 \equiv -\lim_{\mu\to\infty}\frac{1}{2\mu}\nabla_2^2 \tag{40}$$

which, after the infinite-mass limit has been taken, is the null operator acting on the space of electron 2.

Let $\mathbf{r}_1$ and $\mathbf{r}_2$ locate the particles relative to the nucleus, whose atomic number is Z. The three interparticle distances are $r_1\equiv|\mathbf{r}_1|$, $r_2\equiv|\mathbf{r}_2|$, and $r_3\equiv|\mathbf{r}_1-\mathbf{r}_2|$. Together the two particles inhabit the subspace spanned by those eigenvectors of the nonsymmetric Hamiltonian,

$$H_1 \equiv -\frac{1}{2\mu}\nabla_1^2-\frac{Ze^2}{r_1}+0_2\,, \tag{41}$$

that have eigenvalues less than $e_{\max}$. The exact eigenvalue spectrum of H_1 is the (unshifted) spectrum of a hydrogenlike ion with atomic number Z, with one difference: the spectrum of H_1 is infinitely degenerate owing to the inclusion of 0_2, whose eigenvalues are all zero. It is useful to give a system whose Hamiltonian is of the form H_1 a name; we call it ''etherium,'' which connotes the etherial nature of one of the constituents. In practice, when the Hamiltonian of etherium is represented on a finite basis, the degeneracy is finite and imperfect, but nevertheless unambiguous.

We can reduce the Hamiltonian of etherium to a bidiagonal $(L+1)\times(L+1)$ matrix of differential operators which governs the internal motion. Thus, following earlier work [22], we find that H_1 reduces to an $(L+1)\times(L+1)$ matrix h_1 whose rows and columns are each labeled by a pair of indices (l_1,l_2) with $l_1+l_2=L$, whose diagonal elements are

$$h_1(l_1,l_2|l_1,l_2)\equiv-\frac{1}{2}\left[\frac{\partial^2}{\partial r_1^2}+\frac{2}{r_1}\frac{\partial}{\partial r_1}+\frac{\partial^2}{\partial r_3^2}+\frac{2}{r_3}\frac{\partial}{\partial r_3}+\left(\frac{r_1^2-r_2^2+r_3^2}{r_1 r_3}\right)\frac{\partial^2}{\partial r_1\partial r_3}\right]-\frac{Z}{r_1}-\frac{l_1}{r_1}\frac{\partial}{\partial r_1}-\frac{l_1}{r_3}\frac{\partial}{\partial r_3}, \tag{42}$$

whose codiagonal elements are

$$h_1(l_1-1,l_2+1|l_1,l_2)\equiv\frac{l_1}{r_3}\frac{\partial}{\partial r_3}, \tag{43}$$

and whose remaining elements vanish, i.e.,

$$h_1(l_1',l_2'|l_1,l_2) \equiv 0 \quad \text{unless} \quad \begin{cases}\text{either} & l_1'=l_1 \ \text{ and } \ l_2'=l_2\\ \text{or} & l_1'=l_1-1 \ \text{ and } \ l_2'=l_2+1.\end{cases}$$

The matrix representation of each block of h_1 must be constructed on a basis composed of both symmetric and antisymmetric functions since H_1—and h_1—are asymmetric under particle interchange.

Let $|e_n;1\rangle$ be an eigenvector of H_1 with eigenvalue e_n. We can express this eigenvector as the sum of two kets, one symmetric and the other *a*ntisymmetric under particle interchange:

$$|e_n;1\rangle=|e_n;\mathrm{s}\rangle+|e_n;\mathrm{a}\rangle. \tag{44}$$

If H_2 is the Hamiltonian obtained from H_1 by interchanging particles 1 and 2 the ket,

$$|e_n;2\rangle=|e_n;\mathrm{s}\rangle-|e_n;\mathrm{a}\rangle\,, \tag{45}$$

is an eigenvector of H_2 with the same eigenvalue e_n. Without loss of generality we choose the eigenkets to be orthonormal, i.e.,

$$\langle e_m;i|e_n;i\rangle=\delta_{mn} \tag{46}$$

for $i=1,2$. Since $\langle e_m;\mathrm{s}|e_n;\mathrm{a}\rangle=0$ for all m and n we have

$$\langle e_m;\mathrm{s}|e_n;\mathrm{s}\rangle+\langle e_m;\mathrm{a}|e_n;\mathrm{a}\rangle=\delta_{mn}\,. \tag{47}$$

The projection operator that projects onto those states of etherium in which electron 1 is bound with energy less than $e_{\max}$ is

$$P_1(e_{\max}) = \sum_{e_m<e_{\max}} |e_m;1\rangle\langle e_m;1| = \sum_{e_m<e_{\max}} \begin{pmatrix} |e_m;\mathrm{s}\rangle\langle e_m;\mathrm{s}| & |e_m;\mathrm{s}\rangle\langle e_m;\mathrm{a}| \\ |e_m;\mathrm{a}\rangle\langle e_m;\mathrm{s}| & |e_m;\mathrm{a}\rangle\langle e_m;\mathrm{a}| \end{pmatrix}, \tag{48}$$

where this matrix acts on the union of the subspaces spanned by the symmetric and antisymmetric base kets. Interchanging particles 1 and 2 gives

$$P_2(e_{\max}) = \sum_{e_m<e_{\max}} \begin{pmatrix} |e_m;\mathrm{s}\rangle\langle e_m;\mathrm{s}| & -|e_m;\mathrm{s}\rangle\langle e_m;\mathrm{a}| \\ -|e_m;\mathrm{a}\rangle\langle e_m;\mathrm{s}| & |e_m;\mathrm{a}\rangle\langle e_m;\mathrm{a}| \end{pmatrix}. \tag{49}$$

The sum

$$P_1(e_{\max}) + P_2(e_{\max}) = 2\sum_{e_m<e_{\max}} \begin{pmatrix} |e_m;\mathrm{s}\rangle\langle e_m;\mathrm{s}| & 0 \\ 0 & |e_m;\mathrm{a}\rangle\langle e_m;\mathrm{a}| \end{pmatrix} \tag{50}$$

acts on the space of two-electron states, and is symmetric (under interchange of the two electrons) but it is not, in general, a projection operator since those states in which both electrons have energy less than $e_{\max}$ are counted twice. Such states are selected by the product

$$P_1(e_{\max})P_2(e_{\max}) = \sum_{e_m<e_{\max}} \sum_{e_n<e_{\max}} \begin{pmatrix} |e_m;\mathrm{s}\rangle\langle e_m;\mathrm{s}| & |e_m;\mathrm{s}\rangle\langle e_m;\mathrm{a}| \\ |e_m;\mathrm{a}\rangle\langle e_m;\mathrm{s}| & |e_m;\mathrm{a}\rangle\langle e_m;\mathrm{a}| \end{pmatrix} \times \begin{pmatrix} |e_n;\mathrm{s}\rangle\langle e_n;\mathrm{s}| & -|e_n;\mathrm{s}\rangle\langle e_n;\mathrm{a}| \\ -|e_n;\mathrm{a}\rangle\langle e_n;\mathrm{s}| & |e_n;\mathrm{a}\rangle\langle e_n;\mathrm{a}| \end{pmatrix}, \tag{51}$$

which does not, in general, vanish. Carrying through the multiplication on the right side of Eq. (51) gives

$$P_1(e_{\max})P_2(e_{\max}) = \sum_{e_m<e_{\max}} \sum_{e_n<e_{\max}} (\langle e_m;\mathrm{s}|e_n;\mathrm{s}\rangle - \langle e_m;\mathrm{a}|e_n;\mathrm{a}\rangle) \times \begin{pmatrix} |e_m;\mathrm{s}\rangle\langle e_n;\mathrm{s}| & -|e_m;\mathrm{s}\rangle\langle e_n;\mathrm{a}| \\ |e_m;\mathrm{a}\rangle\langle e_n;\mathrm{s}| & -|e_m;\mathrm{a}\rangle\langle e_n;\mathrm{a}| \end{pmatrix}. \tag{52}$$

Since $P_1(e_{\max})$ and $P_2(e_{\max})$ commute [23] and since each matrix on the right sides of Eqs. (48) and (49) is equal to its transpose, the sum of matrices on the right side of Eq. (52) must be equal to its transpose. It follows that the off-diagonal elements of this sum must vanish, and hence

$$P_1(e_{\max})P_2(e_{\max}) = \sum_{e_m<e_{\max}} \sum_{e_n<e_{\max}} (\langle e_m;\mathrm{s}|e_n;\mathrm{s}\rangle - \langle e_m;\mathrm{a}|e_n;\mathrm{a}\rangle) \times \begin{pmatrix} |e_m;\mathrm{s}\rangle\langle e_n;\mathrm{s}| & 0 \\ 0 & -|e_m;\mathrm{a}\rangle\langle e_n;\mathrm{a}| \end{pmatrix}. \tag{53}$$

The symmetric projection operator, which acts on the space of two-electron states and projects onto those states in which at least one electron has energy less than $e_{\max}$, is [20]

$$P(e_{\max}) = P_1(e_{\max}) + P_2(e_{\max}) - P_1(e_{\max})P_2(e_{\max}) \tag{54}$$

and this satisfies

$$P^2(e_{\max}) = P(e_{\max}). \tag{55}$$

Combining Eqs. (50), (53), and (54) gives

$$P(e_{\max}) = 2\sum_{e_m<e_{\max}} \sum_{e_n<e_{\max}} \begin{pmatrix} \delta_{mn}+c_{mn} & 0 \\ 0 & \delta_{mn}-c_{mn} \end{pmatrix} \times \begin{pmatrix} |e_m;\mathrm{s}\rangle\langle e_n;\mathrm{s}| & 0 \\ 0 & |e_m;\mathrm{a}\rangle\langle e_n;\mathrm{a}| \end{pmatrix}, \tag{56}$$

where $2c_{mn} = \langle e_m;\mathrm{a}|e_n;\mathrm{a}\rangle - \langle e_m;\mathrm{s}|e_n;\mathrm{s}\rangle$. It follows from Eqs. (47) and (56) that when $P(e_{\max})$ acts on the symmetric (antisymmetric) subspace only the symmetric (antisymmetric) parts of the eigenvectors of H_1 need to be constructed. When the number of terms contained in the double sum on the right side of Eq. (56) exceeds the dimension of the basis it may be more efficient to evaluate $P(e_{\max})$ using

$$P(e_{\max}) = \frac{3}{2}[P_1(e_{\max}) + P_2(e_{\max})] - \frac{1}{2}[(P_1(e_{\max}) + P_2(e_{\max})]^2 \tag{57}$$

$$= 3\sum_{e_n<e_{\max}} \begin{pmatrix} |e_n;\mathrm{s}\rangle\langle e_n;\mathrm{s}| & 0 \\ 0 & |e_n;\mathrm{a}\rangle\langle e_n;\mathrm{a}| \end{pmatrix} - 2\left[\sum_{e_n<e_{\max}} \begin{pmatrix} |e_n;\mathrm{s}\rangle\langle e_n;\mathrm{s}| & 0 \\ 0 & |e_n;\mathrm{a}\rangle\langle e_n;\mathrm{a}| \end{pmatrix}\right]^2, \tag{58}$$

since the number of operations is fewer.

It is unnecessary to diagonalize the entire matrix representation of H_1; only those eigenvectors with eigenvalues less than $e_{\max}$ are needed. Nevertheless, when the basis is large, the number of eigenvectors with eigenvalues below $e_{\max}$ may

be so large that the work entailed in obtaining them is demanding. This task can be mitigated, or avoided altogether, by expressing the projection operator $P_1(e_{\max})$ as

$$P_1(e_{\max})=\frac{1}{2\pi i}\oint_{\mathcal{C}} dE\,G_1(E), \tag{59}$$

where $G_1(E)=(E-H_1)^{-1}$, where $\mathcal{C}$ is a counterclockwise contour which encloses those poles of $G_1(E)$ that correspond to the bound states of the residual one-electron system with energy eigenvalues less than $e_{\max}$, and where for the moment we assume that $e_{\max}<0$. (The contour $\mathcal{C}$ must exclude the other bound-state poles as well as the cut along the positive real energy axis. We consider the case $e_{\max}>0$ shortly.) Equation (59) can be verified by expressing $G_1(E)$ in terms of its spectral decomposition and performing the integration over E using Cauchy's residue theorem.

Suppose that H_1 can be approximated by a Hamiltonian $\tilde{H}_1$ whose eigenvalues $\tilde{e}_n$ and eigenvectors $|\tilde{e}_n;1\rangle$ can be found easily. For example, $\tilde{H}_1$ might be a tridagonal matrix. We can use Eq. (59) to obtain a tractable approximation to $P_1(e_{\max})$, provided that $\tilde{W}_1=H_1-\tilde{H}_1$ can be regarded as a weak perturbation. Writing $\tilde{G}_1(E)=(E-\tilde{H}_1)^{-1}$, we have

$$G_1(E)=\tilde{G}_1(E)+\tilde{G}_1(E)\tilde{W}_1\tilde{G}_1(E)+\cdots. \tag{60}$$

Substituting the right side of Eq. (60) for $G_1(E)$ on the right side of Eq. (59) and integrating over E gives through first order in $\tilde{W}_1$,

$$\begin{aligned}P_1(e_{\max})\approx \sum_{e_n<e_{\max}} \{&|\tilde{e}_n;1\rangle\langle\tilde{e}_n;1|+\tilde{G}_1(e_n)\\ &\times[\tilde{W}_1-(\tilde{W}_1)_{nn}]|\tilde{e}_n;1\rangle\langle\tilde{e}_n;1|+|\tilde{e}_n;1\rangle\\ &\times\langle\tilde{e}_n;1|[\tilde{W}_1-(\tilde{W}_1)_{nn}]\tilde{G}_1(e_n)\},\end{aligned} \tag{61}$$

where

$$(\tilde{W}_1)_{mn}=\langle\tilde{e}_m;1|\tilde{W}_1|\tilde{e}_n;1\rangle. \tag{62}$$

Suppose further that the domains of H_1 and $\tilde{H}_1$ are the same, so that we can write

$$\tilde{W}_1=\sum_m\sum_n |\tilde{e}_m;1\rangle(\tilde{W}_1)_{mn}\langle\tilde{e}_n;1|. \tag{63}$$

Equation (61) becomes

$$\begin{aligned}P_1(e_{\max})\approx &\sum_{e_n<e_{\max}} |\tilde{e}_n;1\rangle\langle\tilde{e}_n;1|\\ &+\sum_{e_m<e_{\max}}\sum_{e_n>e_{\max}}\frac{(\tilde{W}_1)_{mn}}{e_m-e_n}(|\tilde{e}_m;1\rangle\langle\tilde{e}_n;1|\\ &+|\tilde{e}_n;1\rangle\langle\tilde{e}_m;1|).\end{aligned} \tag{64}$$

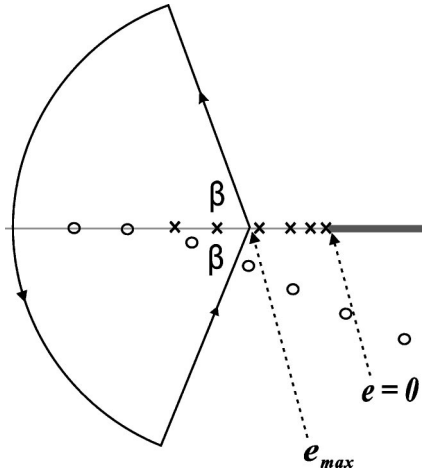

FIG. 1. The contour to be used in constructing a projection operator that projects onto a two-particle subspace, in which one of the particles is bound with energy below $e_{\max}<0$ by an attractive center of force. The crosses mark the bound-state poles of the resolvent for "etherium" and the circles mark the (unshifted) bound- and quasibound-state poles of the resolvent for the complete system composed of two identical light particles (electrons) moving in the field of a stationary infinitely massive nucleus. The thick line represents the overlapping branch cuts of the resolvents.

Equation (64), which is correct through first order in $\tilde{W}_1$, can be extended to higher orders with some straightforward algebra.

We can avoid altogether finding the eigenvectors of etherium by performing the contour integration on the right side of Eq. (59). Let us choose $\mathcal{C}$ to be the boundary of the sector $\pi-\beta\leqslant|\arg(E)|\leqslant\pi$, where β is a fixed angle in the range $0<\beta<\pi$; thus, as shown in Fig. 1, $\mathcal{C}$ consists of two lines, $E=e_{\max}+se^{\pm i(\pi-\beta)}$ with $0\leqslant s<\infty$, which originate at $e_{\max}$ and are joined at infinity by an arc. The integration over the infinite arc can be performed immediately to give

$$P_1(e_{\max})=\frac{\beta}{\pi}-\mathrm{Im}\,\frac{e^{-i\beta}}{\pi}\int_0^\infty ds\,G_1(e_{\max}-e^{-i\beta}s). \tag{65}$$

The contribution from the integral over s should not change as we move $e_{\max}$ up the negative real axis beyond the energy of the last accessible bound state. However, this contribution will change if we move $e_{\max}$ past the origin since there is a branch point at the origin; recall that the contour $\mathcal{C}$ must not cross the cut along the positive energy axis. To evaluate the integral we make use of the $1/E$ expansion of $G_1(E)$, applicable for values of E far from the cut along the postive real E axis:

$$G_1(E)=\frac{1}{E}\sum_{n=0}^{\infty}\left(\frac{H_1}{E}\right)^n. \tag{66}$$

Introducing a sufficiently large real positive number s_∞, larger than $e_{\max}$, we obtain

$$\begin{aligned}\mathrm{Im}\, e^{-i\beta}\int_{s_\infty}^{\infty} ds G_1(e_{\max}-e^{-i\beta}s)&\\ =\mathrm{Im}\int_{s_\infty}^{\infty} ds\sum_{n=0}^{\infty}\frac{e^{in\beta}}{(e_{\max}e^{i\beta}-s)^{n+1}}H_1^n&\\ =\tan^{-1}\left(\frac{e_{\max}\sin\beta}{s_\infty-e_{\max}\cos\beta}\right)-\mathrm{Im}\sum_{n=1}^{\infty}\frac{e^{in\beta}H_1^n}{n(e_{\max}e^{i\beta}-s_\infty)^n}.&\end{aligned} \tag{67}$$

When H_1 and its powers are sandwiched inside matrix elements, the sum becomes a normal asymptotic series, whose convergence can be improved by the Padé summation [28]. To integrate over the interval $[s_0,s_\infty]$, where s_0 is a small number in the range $0<s_0<s_\infty$, we use

$$G_1(E)=-i\int_0^\infty dt e^{i(E-H_1)t} \tag{68}$$

to write

$$\begin{aligned}e^{-i\beta}\int_{s_0}^{s_\infty} ds G_1(e_{\max}-e^{-i\beta}s)&\\ =\int_0^\infty dt\left(\frac{e^{-ie^{-i\beta}(s_\infty-s_0)t}-1}{t}\right)e^{i(e_{\max}-H_1)t}e^{-ie^{-i\beta}s_0t}.&\end{aligned} \tag{69}$$

The integrand on the right side of Eq. (69) is nonsingular at $t=0$ and is damped exponentially, by the factor $e^{-s_0t\sin\beta}$, at large t. The propagator $e^{i(e_{\max}-H_1)t}$ can be evaluated efficiently as described earlier [13]. We can extend the integration from s_0 to 0 by making a Taylor-series expansion in powers of s_0; derivatives with respect to s_0 simply yield powers of t in the integrand on the right side of Eq. (69).

The symmetric operator $P(e_{\max})$ projects onto states in which at least one electron has an energy below $e_{\max}$, but we often need an operator, denoted by $P(e_a,e_b)$, which projects onto states in which one electron has an energy in the interval $[e_a,e_b]$. To construct $P(e_a,e_b)$ we replace $P_i(e_{\max})$ for $i=1,2$ in Eq. (54) or (57) by

$$P_i(e_a,e_b)\equiv P_i(e_b)-P_i(e_a), \tag{70}$$

where $P_i(e)$ has the meaning used above. This replacement amounts to replacing the range of the sum in Eq. (48) or (49) from $e_m<e_{\max}$ to $e_a<e_m<e_b$, or, equivalently, it amounts to choosing the contour of integration $\mathcal{C}$ in Eq. (59) so that it encloses only those poles in the interval $[e_a,e_b]$. Note that, in general, $P(e_a,e_b)\neq P(e_b)-P(e_a)$.

In the preceding section we introduced symmetric operators that project onto orthogonal subspaces correpsonding to different channels or groups of subchannel. Let α and α' label subchannels in which one of the electrons has energy in the intervals $[e_a,e_b]$ and $[e_c,e_d]$, respectively. Assume these energy intervals to be nonoverlapping. Writing $P_{i\alpha}=P_i(e_a,e_b)$ and $P_{i\alpha'}=P_i(e_c,e_d)$, for $i=1,2$, the operators

$$R_\alpha=P_{1\alpha}+P_{2\alpha}-P_{1\alpha}P_{2\alpha}, \tag{71}$$

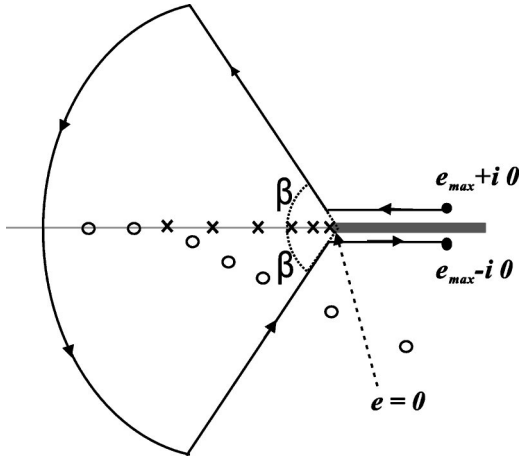

FIG. 2. Same as Fig. 1 but with $e_{\max}>0$.

$$R_{\alpha'}=P_{1\alpha'}+P_{2\alpha'}-P_{1\alpha'}P_{2\alpha'} \tag{72}$$

project onto subspaces corresponding to the (sub)channels α and α'. However, these subspaces are not orthogonal; in general, $P_{i\alpha}P_{j\alpha'}\neq 0$ for $i\neq j$, although $P_{i\alpha}P_{i\alpha'}=0$, since the energy intervals $[e_a,e_b]$ and $[e_c,e_d]$ do not overlap. Hence, noting that $P_{i\alpha}$ and $P_{j\alpha'}$ commute, we subtract $P_{1\alpha}P_{2\alpha'}+P_{2\alpha}P_{1\alpha'}$ to define the orthogonal projection operators

$$P_\alpha=R_\alpha-R_\alpha R_{\alpha'}, \tag{73}$$

$$P_{\alpha'}=R_{\alpha'}-R_{\alpha'}R_\alpha. \tag{74}$$

The subtraction, reflected by the last terms on the right sides of Eqs. (73) and (74), leads to orthogonality by ensuring that neither electron in subchannel α has an energy in the interval $[e_c,e_d]$; and neither electron in subchannel α' has an energy in the interval $[e_a,e_b]$. The exclusion of the electrons in one (sub)channel from the energy range specified by the index of an orthogonal (sub)channel is consistent with energy conservation for open (sub)channels. This exclusion does, however, reduce the dimension of each subspace onto which P_α and $P_{\alpha'}$ project; indeed, if we were to make the, admittedly unphysical, choice of $P_{i\alpha'}=1-P_{i\alpha}$, for $i=1,2$, we would have $P_\alpha=P_{1\alpha}P_{2\alpha}$ and $P_{\alpha'}=P_{1\alpha'}P_{2\alpha'}$, since the electrons would have no option but to each have an energy in the same energy range, the range specified by the appropriate (sub)channel index.

To treat the total breakup of the system we must allow $e_{\max}$ to become positive, which we can do by letting the contour $\mathcal{C}$ run along the upper and lower edges of the cut, as shown in Fig. 2. Integration along the cut can be performed by expressing $G_1(E)$ in terms of its series representation. Let E_{xs} denote the excess energy of the system above the total breakup threshold. The operator $P_1(0,\frac{1}{2}E_{\mathrm{xs}})$ projects onto a subchannel in which electron 1 is liberated with energy in the range $0-\frac{1}{2}E_{\mathrm{xs}}$; electron 2 necessarily (by energy conservation) has an energy in the range $\frac{1}{2}E_{\mathrm{xs}}-E_{\mathrm{xs}}$. The energy distribution can be calculated from the derivative $(d/de)P_1(0,e)=-(1/\pi)\mathrm{Im}\, G_1(e)$.

TABLE I. Total cross sections (in units πa_0^2) for ^1S-wave elastic scattering of an electron from a ground-state hydrogen atom at impact energies below the inelastic thresholds and above the ionization threshold. The last column contains present results.

Energy (Ry)	$\sigma(1s)$	$\sigma(1s)$	$\sigma(1s)$
0.04	77.31 [a]	77.75 [b]	77.95
0.09	43.75 [a]	43.81 [b]	43.77
0.16	24.40 [a]	24.36 [b]	24.42
0.25	13.92 [a]	13.86 [b]	13.93
0.36	8.27 [a]	8.22 [b]	8.23
0.49	5.25 [a]	5.21 [b]	5.28
1.21	1.13 [c]	0.916 [b]	1.29
1.44	0.912 [c]	1.196 [b]	0.928
1.80		0.672 [b]	0.555
2.25	0.495 [c]	0.508 [b]	0.506

[a]Schwartz [24].
[b]Scholz *et al.* [27].
[c]Callaway [26].

IV. TEST RESULTS

We have performed various tests of the method outlined in the previous sections, and in this section we present some results for a system composed of two electrons and a proton. We took the proton to be infinitely massive and at rest. Our calculations were performed on a single-processor (Pentium 4, 1.7 GHz) desktop with 1.25 Gbyte of internal memory and ample disk space (40 Gbyte) to accomodate all matrices.

To treat electron scattering from a hydrogen atom we used independent particle coordinates, $\mathbf{r}_1$ and $\mathbf{r}_2$, and a (real) basis composed of the symmetrized functions

$$e^{-k(r_1+r_2)}r_1^{l_1}r_2^{l_2}L_{m-l-1}^{2l+1}(2kr_1)L_{n-l-1}^{2l+1}(2kr_2)\mathcal{Y}_{LM}^{(l_1l_2)}(\hat{\mathbf{r}}_1,\hat{\mathbf{r}}_2) \pm 1\leftrightarrow 2,$$

where the sign is + (−) for singlet (triplet) states. Here $\mathcal{Y}_{LM}^{(l_1l_2)}(\hat{\mathbf{r}}_1,\hat{\mathbf{r}}_2)$ is an eigenfunction of the total orbital angular momentum operator $\hat{\mathbf{L}}^2$ and its projection $\hat{L}_z$ along the polar axis (the z axis), and it is obtained by coupling the spherical harmonics $Y_{l_1m}(\hat{\mathbf{r}}_1)$ and $Y_{l_2,M-m}(\hat{\mathbf{r}}_2)$ with $|l_1-l_2|\leqslant L\leqslant l_1+l_2$. We considered only ^1S-wave scattering, with the atom initially in the ground state, so we put $L=M=0$ and $l_1=l_2$. We imposed the restriction $l_1,l_2\leqslant 3$. We allowed the (single) length scale, $1/k$, of the basis to take on three values, i.e. $k=$ 0.4, 0.5, or 0.7 a.u., and chose the value most appropriate for the impact energy. We let the indices m and n of the Laguerre polynomials $L_m(2kr_1)$ and $L_n(2kr_2)$ each run from 0 to 39 with $m\leqslant n$. The dimension of this basis is 3280. The initial-state wave function is a symmetrized product of a plane wave and a ground-state hydrogen atom wave function, and the perturbation in the entrance channel is the interaction between the incident electron and the hydrogen atom.

In Tables I and II, and Fig. 3, we show results for elastic and inelastic scattering. In general, we find good agreement with other results, although less so at energies not far above the complete breakup threshold, i.e., the region 1.21–1.80 Ry. In the region between the $n=2$ and $n=3$ excitation thresholds, where there are Feshbach resonances, we compare with the benchmark results of Bartschat *et al.* which are accurate to better than 1%. Our results agree to within 1% with those of Bartschat *et al.*

TABLE II. Total cross sections (in units πa_0^2) for excitation of a hydrogen atom, summed over the 2s and 2p levels, by ^1S-wave electron impact at moderate energies above the ionization threshold. The last column contains present results.

Energy (Ry)	$\sigma(2s+2p)$	$\sigma(2s+2p)$	$\sigma(2s+2p)$
1.21	0.198 [a]	0.155 [b]	0.174
1.44	0.130 [a]	0.124 [b]	0.128
1.80		0.0891 [b]	0.0820
2.25	0.0649 [a]	0.0609 [b]	0.0615

[a]Callaway [26].
[b]Scholz *et al.* [27].

Now we turn to photodetachment of H^-. To treat this process we used perimetric coordinates u, v, and w, defined as [29]

$$u=r_2+r_3-r_1, \tag{75}$$

$$v=r_1+r_3-r_2, \tag{76}$$

$$w=2(r_1+r_2-r_3). \tag{77}$$

The orientation of the system can be specified by the three Euler angles. Alternatively, we can use the four angles θ_1,

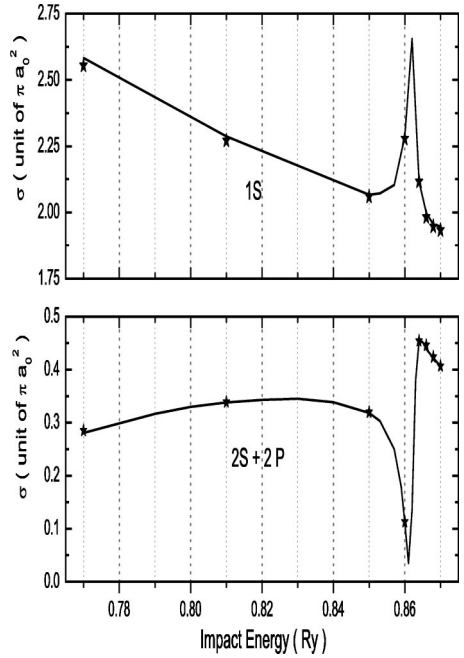

FIG. 3. Partial cross sections for elastic scattering (upper box) and excitation to the $n=2$ level (lower box) at energies in the region of a Feshbach resonance. The stars are the results of Bartschat *et al.* [25], and the solid lines are the present results.

ϕ_1, θ_2, and ϕ_2 which are the polar and azimuthal angles of $\mathbf{r}_1$ and $\mathbf{r}_2$, respectively; only three of these angles are independent since they are related through r_3. The complete symmetrized basis functions are

$$\Phi_{lmn}^{Ll_1l_2}(\mathbf{r}_1,\mathbf{r}_2;\pm)=\Phi_{lmn}^{Ll_1l_2}(\mathbf{r}_1,\mathbf{r}_2)\pm 1\leftrightarrow 2, \tag{78}$$

where $l_1+l_2=L$ and where, introducing $\zeta_1=\sin(\theta_1)e^{i\phi_1}$, $\zeta_2=\sin(\theta_2)e^{i\phi_2}$, and the angular-momentum lowering operator $\hat{L}_-$, the *un*symmetrized basis functions are [30]

$$\Phi_{lmn}^{Ll_1l_2}(\mathbf{r}_1,\mathbf{r}_2) = \frac{1}{\sqrt{(2L)!}}[(\hat{L}_-)^L(r_1\zeta_1)^{l_1}(r_2\zeta_2)^{l_2}]\phi_{lmn}(r_1,r_2,r_3), \tag{79}$$

where

$$\phi_{lmn}(r_1,r_2,r_3) = e^{-1/2(k_1u+k_2v+k_3w)}L_l(k_1u)L_m(k_2v)L_n(k_3w). \tag{80}$$

Note that $\Phi_{lmn}^{Ll_1l_2}(\mathbf{r}_1,\mathbf{r}_2)$ has parity $(-1)^L$ and is an eigenfunction of $\hat{\mathbf{L}}^2$ and $\hat{L}_z$, with eigenvalues $L(L+1)$ and 0, respectively. In principle, this basis has three length scales, but in practice care must be taken to preclude linear dependence if k_1 is chosen to be different from k_2. Rather than choose k_1 and k_2 to be different, we accomodate more than one length scale by using a basis set that is composed from a combination of subsets, where each subset spans a distinct (almost orthogonal) subspace corresponding to a particular subchannel or group of subchannels. Each subset is assigned a single length scale $k(=k_1=k_2=k_3)$ with the value of k chosen to be appropriate to the subchannel (or group of subchannels) described; since different subsets do not overlap significantly, the problem of linear dependence does not arise. In the calculations reported on here we used a combination of two subsets, one ($k=0.70$ a.u.) spanning the subspace corresponding to the subchannel in which the hydrogen atom is left in the ground state, and the other ($k=0.19$ a.u.) spanning the remainder of the vector space. Note that $\phi_{lmn}(r_1,r_2,r_3)=\phi_{mln}(r_2,r_1,r_3)$ when $k_1=k_2$; hence we imposed the restrictions $l_1<l_2$ if $l_1\neq l_2$ and $l\leqslant m$ if $l_1=l_2$, to avoid linear dependence between $\Phi_{lmn}^{Ll_1l_2}(\mathbf{r}_1,\mathbf{r}_2;\pm)$ and $\Phi_{mln}^{Ll_2l_1}(\mathbf{r}_1,\mathbf{r}_2;\pm)$. Since we considered photodetachment by one linearly polarized photon, we put $L=M=0$ for the ground state of H^- and and $L=1$ and $M=0$ for the response function. The dimension of the basis used to describe the response function was 4000. A smaller basis, of dimension about 2000, was used to describe the wave function of the negative ion. The initial-state wave function describes the ground state of the negative ion, and the perturbation in the entrance channel is the dipole interaction (in the velocity gauge) between the negative ion and the monochromatic electric field.

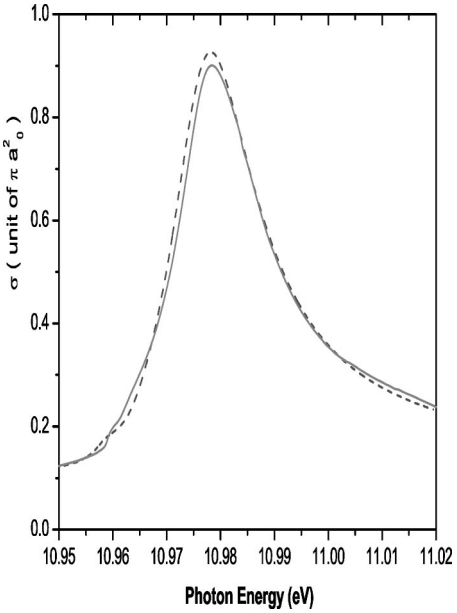

FIG. 4. Total cross section for photodetachment of H^- in the region of a shape resonance. The solid line was obtained using the present method, while the broken line was obtained using a complex basis in conjunction with a standard expression for the total decay rate.

In Fig. 4 we show the total cross section for photodetachment of H^- over a range of photon energies—from 10.95 eV, just below the threshold (10.9595 eV) for $n=2$ excitation of the residual hydrogen atom, to 11.02 eV, beyond the shape resonance centered at about 10.98 eV. As a check on the present method we carried out an additional, very different, calculation which employed a *complex* basis [31] in conjunction with the standard expression $-2\mathrm{Im}\langle\psi|V^\dagger G(E)V|\psi\rangle$ for the total photodetachment rate, where $|\psi\rangle$ is the ground-state eigenket for H^-. The comparison between both sets of results shown in Fig. 4 is reassuring. The total cross section rises sharply as the excitation threshold is approached, exhibits a slight hump in the vicinity of the threshold, and falls quite sharply above the shape resonance.

We have also used the present method to estimate partial cross sections for photodetachment to the $n=1$ and $n=2$ subchannels. We were unable to obtain numerically stable results at photon energies immediately above the threshold, but we obtained reasonably stable results beyond 2 or 3 meV in excess of the threshold. To cover the 1.5-meV region extending from the threshold (10.9595 eV) to 10.961 eV we used interpolation, setting the $n=2$ partial cross section to zero at (and below) the threshold. Our smoothed results are shown in Fig. 5. The shape resonance originates in the $n=2$ subchannel; it is broad, and strongly influences the cross section over a wide range of energies, even below the threshold where the $n=2$ subchannel is closed. Indeed, we see that the $n=1$ partial cross section rises sharply just below the threshold, but falls sharply just above the threshold where the $n=2$ partial cross section rises sharply. In contrast, the total cross section (Fig. 4) varies quite smoothly through threshold, exhibiting only a slight hump, since the sharp fall in the $n=1$ partial cross section is offset by the sharp rise in

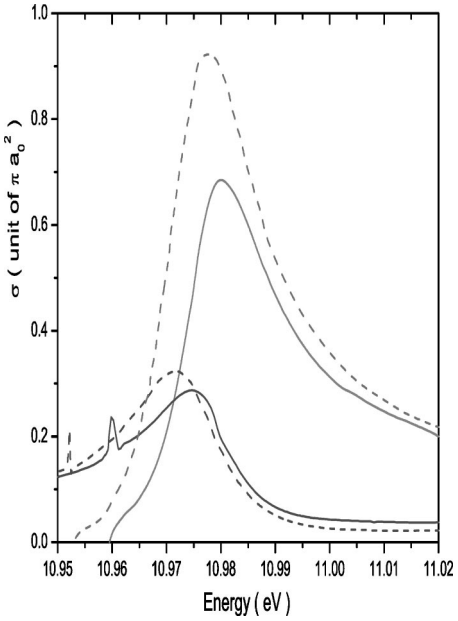

FIG. 5. Partial cross sections for photodetachment of H^- in the region of the shape resonance; the residual hydrogen atom is left in its ground ($n=1$) or first excited ($n=2$) state. The broken lines are the results of Sadeghpour *et al.* [35] and the solid lines are our results. Upper (lower) curves are for the $n=2$ ($n=1$) subchannel.

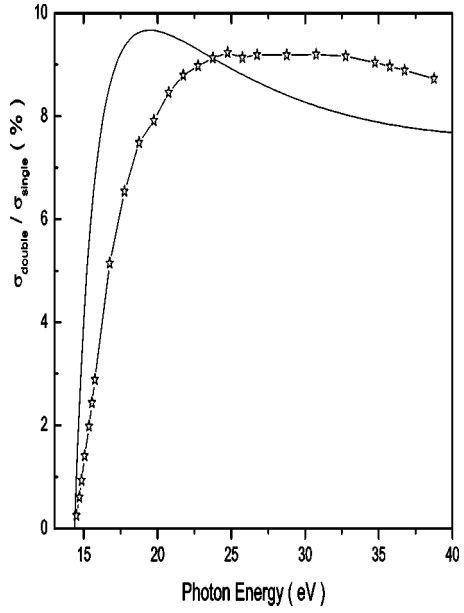

FIG. 6. Ratio of the double- to single-electron escape cross sections for one-photon absorption by H^-. The stars are the results of Kheifets and Bray [36] and the solid lines are our results.

the $n=2$ partial cross section. Evidently, the $n=1$ and $n=2$ subchannels are strongly coupled by the shape resonance. Calculations of partial cross sections in the shape-resonance region have been performed by several other groups, but agreement among results is less than perfect—see, e.g., Refs. [32–35]. For comparison with our results we show the more recent data of Sadeghpour *et al.* [35]. The agreement is fair, but again not perfect. The agreement on the background is good, but the heights of the peaks, particularly, the height of the $n=2$ peak, differ; our estimates of the peak heights are smaller, and are in better agreement with those estimated by Broad and Reinhardt [33], whose results are not shown. Note that Sadeghpour *et al.* [35] found a spike in the $n=1$ partial cross section close to threshold, similar to the spike we observed, but they attributed this spike to one of the dipole resonances accumulating at the threshold from below. As mentioned above, we attribute the spike to the strong coupling of the $n=1$ and $n=2$ subchannels by the shape resonance; if it were due to a dipole resonance one would expect it to be distinctly visible in the total cross section.

Finally, in Fig. 6 we show results for two-electron escape from H^- by one-photon absorption, for photon energies extending from the double-escape threshold (14.3608 eV) to 40 eV. Other results in this energy range include those of Kheifets and Bray [36] and Meyer *et al.* [37], which agree rather well with each other. We show the ratio of the (integrated) cross sections for double- and single-electron escape, and we compare our results to the (velocity-gauge) results of Kheifets and Bray [36].

V. CONCLUSION

We have described a method, based on the analyticity of the resolvent $G(E)$ with respect to its underlying time scale, to treat three-body collisions, and we have tested the method by applying it to electron scattering and photodetachment. The most severe approximation entailed in the method is the truncation of the infinite dimensional space on which $G(E)$ acts to a large but finite-dimensional vector space spanned by a set of real basis functions. Within this finite space, smaller subspaces are selected by projection operators P_α which map onto open (sub)channels. The partial resolvents $P_\alpha G_\alpha(E) P_\alpha$, where $G_\alpha(E)=1/(E-P_\alpha H P_\alpha)$, act on these smaller subspaces, and they can be constructed from series representations using stable recurrence relations. The resolvent acting on the full space spanned by the (finite) basis can be obtained by solving a (complex symmetric) linear system using a generalization of the Cholesky decomposition for real, positive definite, symmetric matrices. The most computer-intensive parts of the method are the construction of the projection operators and the subsequent solution of the linear system. Although it is unnecessary to diagonalize large matrices, the solution of the linear system is greatly simplified if the large matrix QHQ, where $Q=1-\Sigma_\alpha P_\alpha$, is diagonalized. Our test calculations of cross sections for ^1S-wave electron scattering from a hydrogen atom, and photodetachment of the negative hydrogen ion, gave results in reasonable agreement with those achieved using current state-of-the-art methods; we hope to provide further evidence of the utility of the method in the future. We plan to make several refinements; in particular, we plan to incorporate the method in a variational principle [38].

ACKNOWLEDGMENTS

During the early stages of this project we benefited from the exploratory work of Wenyu Liu, and it is a pleasure to record our gratitude to him. R.S. gratefully acknowledges support from the NSF, under Grant No. PHY-0070936.

[1] *Atomic and Molecular Processes: An R-Matrix Approach*, edited by P.G. Burke and K.A. Berrington (Institute of Physics, Philadelphia, 1993).
[2] E.J. Heller and H.A. Yamani, Phys. Rev. A **9**, 1209 (1974).
[3] J. Callaway and K. Unnikrishnan, J. Phys. B **26**, L419 (1993).
[4] I. Bray and A. Stelbovics, Phys. Rev. A **46**, 6995 (1992).
[5] M. Baertschy, T.N. Rescigno, W.A. Isaacs, X. Li, and C.W. McCurdy, Phys. Rev. A **63**, 022712 (2001).
[6] H. Bachau, E. Cormier, P. Decleva, J.E. Hansen, and F. Martin, Rep. Prog. Phys. **64**, 1815 (2001).
[7] M.S. Pindzola and F.J. Robicheaux, Phys. Rev. A **61**, 052707 (2000).
[8] L.A.A. Nikolopoulos and P. Lambpropoulos, J. Phys. B **34**, 545 (2001).
[9] J.S. Parker *et al.*, J. Phys. B **34**, L69 (2001).
[10] T. Mercouris, C. Haritos, and C.A. Nicolaides, J. Phys. B **34**, 3789 (2001).
[11] J. Colgan and M.S. Pindzola, Phys. Rev. Lett. **88**, 173002 (2002).
[12] T. Geyer and J.M. Rost, J. Phys. B **35**, 1479 (2002).
[13] R. Shakeshaft and B. Piraux, Adv. Theor. Math. Phys. **4**, 1093 (2000).
[14] R. Shakeshaft, Phys. Rev. A **62**, 062705 (2000).
[15] R. Shakeshaft, Phys. Rev. A **66**, 012506 (2002).
[16] M. Abramowitz and I.E. Stegun, *Handbook of Mathematical Functions* (U.S. GPO, Washington, D.C., 1964).
[17] F.A. McDonald and J. Nuttall, Phys. Rev. Lett. **23**, 361 (1969).
[18] If H is represented by a finite matrix, the expectation value of W must remain small and stable as the size of the matrix (basis) increases.
[19] G.H. Golub and C.F. Van Loan, *Matrix Computations*, 3rd ed. (Johns Hopkins, Baltimore, 1996).
[20] Y. Hahn, T.F. O'Malley, and L. Spruch, Phys. Rev. **128**, 932 (1962); H. Feshbach, Ann. Phys. (N.Y.) **5**, 357 (1958).
[21] R. Shakeshaft, Phys. Rev. A **60**, 1280 (1999); **60**, 4198 (1999).
[22] M. Pont and R. Shakeshaft, Phys. Rev. A **51**, 257 (1995).
[23] The operators $P_1(e_{\max})$ and $P_2(e_{\max})$ commute only approximately unless independent-particle coordinates are used.
[24] C. Schwartz, Phys. Rev. **124**, 1468 (1961).
[25] K. Bartschat, I. Bray, P.G. Burke, and M.P. Scott, J. Phys. B **29**, 5493 (1996).
[26] J. Callaway, Phys. Rev. A **32**, 775 (1985).
[27] T. Scholz, P. Scott, and P.G. Burke, J. Phys. B **21**, L139 (1988).
[28] C.M. Bender and S.A. Orszag, *Advanced Mathematical Methods for Scientists and Engineers* (McGraw-Hill, New York, 1978).
[29] C.L. Pekeris, Phys. Rev. **112**, 1649 (1958).
[30] B. Yang, M. Pont, R. Shakeshaft, E. van Duijn, and B. Piraux, Phys. Rev. A **56**, 4946 (1997).
[31] We used a similar basis, composed of the functions given in Eq. (80), but with the complex wave numbers $k_1=0.2e^{-i\chi}$, $k_2=0.7e^{-i\chi}$, and $k_3=(k_1+k_2)/2$ where $\chi=20°$. The basis size was 4860.
[32] H.A. Hyman, V.L. Jacobs, and P.G. Burke, J. Phys. B **5**, 2282 (1972).
[33] J.T. Broad and W.P. Reinhardt, Phys. Rev. A **14**, 2159 (1976).
[34] C-R. Liu, N-Y. Du, and A.F. Starace, Phys. Rev. A **43**, 5891 (1991).
[35] H.R. Sadeghpour, C.H. Greene, and M. Cavagnero, Phys. Rev. A **45**, 1587 (1992).
[36] A. Kheifets and I. Bray, Phys. Rev. A **58**, 4501 (1998).
[37] K.W. Meyer, C.H. Greene, and B.D. Esry, Phys. Rev. Lett. **78**, 3662 (1997).
[38] E. Gerjuoy, A.R.P. Rau, and L. Spruch, Rev. Mod. Phys. **55**, 725 (1983).